THE ASTROPHYSICAL JOURNAL, 365:532–538, 1990 December 20

OPTICALLY THIN HOT PLASMA NEAR THE GALACTIC CENTER: MAPPING OBSERVATIONS OF THE 6.7 keV IRON LINE

S. YAMAUCHI, M. KAWADA, K. KOYAMA, H. KUNIEDA, AND Y. TAWARA
Department of Astrophysics, School of Science, Nagoya University
AND
I. HATSUKADE
Department of Electronic Engineering, Faculty of Engineering, Miyazaki University
Received 1990 February 26; accepted 1990 June 15

ABSTRACT

We report results of 6.7 keV emission-line mapping observations of the Galactic center region. The 6.7 keV emission line is attributable to a helium-like iron K-shell transition in an optically thin hot plasma of a temperature about 10^8 K. The surface brightness distribution of the plasma is elliptical with a major axis of 1°.8 (FWHM) and an axial ratio of about 0.5. The major axis is tilted about 20° with respect to the Galactic plane. We also determined the total flux and surface brightness of the extended X-ray emission in the continuum X-ray band to be (1–3) $\times 10^{-9}$ ergs s^{-1} cm^{-2} and (2–5) $\times 10^{-6}$ ergs s^{-1} cm^{-2} sr^{-1} in 2–10 keV, respectively. The equivalent width of the iron line is estimated to be 500–1300 eV, consistent with the value expected for a cosmic iron abundance. Several possibilities of the origin of the extended plasma are considered.

Subject headings: galaxies: nuclei — galaxies: The Galaxy — X-rays: sources — X-rays: spectra

I. INTRODUCTION

In the optical window, the Galactic center has been obscured by an enormous amount of dust in the Galactic disk. This "dust curtain" has been removed by the opening of new windows in wave bands other than the optical. Radio and infrared observations have demonstrated that the Galactic center is very bright and complex. Several expanding molecular clouds (or rings) suggest intermittent explosions near the Galactic center, while the infrared observations reveal a high concentration of stellar objects toward the Galactic center (Oort 1977; Genzel and Townes 1987; and references therein). The detection of γ-ray line emission indicates that energetic phenomena, such as large numbers of supernovae or novae, took place near the Galactic center within the last 10^6 yr (Genzel and Townes 1987; and references therein). However, limited photon statistics have been a problem for γ-ray observations. X-ray observations should be more useful to investigate these high-energy phenomena, because they provide us with more photons and better spatial resolution than the γ-ray observations.

Previous X-ray continuum observations of the Galactic center region revealed the presence of several point sources and unresolved diffuse emission (e.g., Watson *et al.* 1981; Skinner *et al.* 1987; Kawai *et al.* 1988). However, the X-ray continuum intensity of the Galactic center has not been particularly strong compared to that of other regions of the Galaxy. Thus, any particularly high activity from the Galactic center region has not been found in the X-ray band, in contrast to the results obtained in the radio, infrared, and γ-ray bands.

Recently, Koyama *et al.* (1989) discovered a remarkable enhancement of the 6.7 keV emission line toward the Galactic center. Since the 6.7 keV line is attributable to helium-like iron in an optically thin hot plasma with a temperature about 10^8 K, this would be the first X-ray indication of activity in the Galactic center region.

We have carried out further two-dimensional mapping of this optically thin hot plasma in the Galactic center using the 6.7 keV iron line. In this paper we report the results of these observations and derived physical parameters and discuss several possibilities for the origin of the optically thin hot plasma. Throughout this paper, we assume that the distance of the Galactic center is 8.5 kpc, and errors quoted are at the 1 σ level.

II. OBSERVATIONS

The observations were made on 1988 March 17 and 1989 April 1–2 and 5–6 with the Large Area Proportional Counters (LAC) on board the X-ray astronomy satellite *Ginga*. The total effective area of the LAC is 4000 cm^2, and its energy range is 2–38 keV. Details of the *Ginga* satellite and the LAC have been given in separate papers (Makino *et al.* 1987; Turner *et al.* 1989). We carried out scanning observations near the Galactic center along several paths parallel to the Galactic plane with a scan speed of about 1° minute^{-1}. In order to increase statistics and minimize background fluctuations, we employed multiple scans (five to 10 scans per day) over the same region. The FWHM of the LAC field of view is about 1° and 2°, along and perpendicular to the scan path, respectively. The accuracy of the attitude determination is better than 0°.1. The data were taken in the 48 energy channel mode for each detector and layer (MPC-1 mode), with a time resolution of 4 s or 16 s. The log of the Galactic center observations is summarized in Table 1.

III. ANALYSIS AND RESULTS

a) *Iron Line Profiles*

We folded the multiple-scan data azimuthally to make five scan profiles with elevation angles from the Galactic plane of $b \cong 1°.7, 0°.5, -0°.6, -1°.1, -2°.1$, then sliced the scan profiles at 0°.4 intervals and constructed the X-ray spectrum. The integration time for each spectrum was more than 100 s. Non–X-ray background and cosmic diffuse X-rays were subtracted using the method given by Awaki *et al.* (1991). We selected several X-ray spectra from regions where no cataloged X-ray source is

TABLE 1

Ginga OBSERVATIONS OF THE GALACTIC CENTER

Date	Scan Area	Observation Mode/ Time Resolution	Scan Speed (degrees per minute)	Number of Scans
1988 Mar 17	$l = -15° \leftrightarrow 20°$, $b = 0.5$	MPC-1/ 4 s	1.38	9
1989 Apr 1	$l = -8° \leftrightarrow 8°$, $b = -1.1$	MPC-1/ 16 s	0.64	5
1989 Apr 2	$l = -8° \leftrightarrow 8°$, $b = -0.6$	MPC-1/ 16 s	0.64	5
1989 Apr 5	$l = -8° \leftrightarrow 8°$, $b = 1.7$	MPC-1/ 4 s	0.95	10
1989 Apr 6	$l = -8° \leftrightarrow 8°$, $b = -2.1$	MPC-1/ 4 s	1.38	10

in the LAC field of view and fitted the spectra with a model, consisting of thermal bremsstrahlung emission plus a narrow emission line. Free parameters are the normalization and the temperature of the thermal bremsstrahlung emission, the intensity and the energy of the line emission, and the hydrogen column density. The intrinsic line width was fixed at 0.05 keV which is smaller than the energy resolution of the LAC. The fits were acceptable with the reduced χ^2 values of 0.67–1.38. The best-fit parameters are listed in Table 2, while the spectral shapes are shown as solid lines in Figure 1. In these spectra, we found a strong emission line at an energy ranging from 6.6 to 6.8 keV. This line is mainly attributable to the K-line transition in helium-like iron. The temperature of the thermal bremsstrahlung emission determined from the continuum shape is in the range of 9–15 keV. Thus we conclude that the extended emission near the Galactic center is likely due to a thin hot plasma with a temperature of about 10 keV.

Although the other regions are contaminated by cataloged point sources, we conducted the same model fit in the limited energy band of 4.5–14 keV in an attempt to improve our knowledge of the distribution of the iron line emission. Except for the data which include bright X-ray point sources (GX 3+1; GX 5−1; MXB 1728−34; a transient source, Makino 1988), the model gave acceptable fits. The intensity distribution of the iron line as a function of the Galactic longitude is given in Table 3 and Figure 2.

We fitted these scan profiles of the iron line intensity with a model of a one-dimensional Gaussian, adding constant background level. The best fit curves are shown in Figure 2, with the peak intensity indicated by arrows. We found that the iron line–emitting region is not a pointlike source but is extended by about 1°–2° (FWHM). This result confirms, with better sensitivity, the extended line emission previously reported by Koyama *et al.* (1989). The existence of the constant background indicates that there is another, more widely distributed, iron line emission source. This component is likely to be the Galactic ridge emission because the iron intensity is the same as that extrapolated from the results of Koyama *et al.* (1986) and Koyama (1989). Further details of the Galactic ridge emission detected with the present scan observations will be given in a separate paper.

b) *Iron Line Distribution*

The intensity peak of the iron line near the Galactic center shows a systematic shift from the Galactic center; a shift toward positive longitude at positive latitude and vice versa. This fact indicates that the emission region is not symmetric with respect to the Galactic plane. In order to estimate the two-dimensional surface brightness distribution of the iron line emission in the Galactic center region, we subtracted the ridge components (as is determined in § III*a*), and we carried out combined fitting to all the scan profiles with a single model having a two-dimensional Gaussian shape. Free parameters of this fitting are the center position, the widths along the major and minor axes, the normalization factor (the total number of photons in the iron line), and the tilting angle with respect to the Galactic plane. The best-fit model of iron line emitting region is illustrated in Figure 3. From this two-dimensional fitting, we found that the emitting region is an elliptical structure tilted $21° \pm 3°$ with respect to the Galactic plane. The angular sizes of the major and minor axes are 1.8 ± 0.1 (FWHM) and 1.0 ± 0.1 (FWHM), respectively. These values correspond to 270 ± 15 pc and 150 ± 15 pc at the Galactic center. The surface brightness at the peak, and the total flux of the iron line from this region, are $(2.2 \pm 0.1) \times 10^{-7}$ ergs s^{-1} cm^{-2} sr^{-1}, $(1.3 \pm 0.1) \times 10^{-10}$ ergs s^{-1} cm^{-2}, respectively. The total luminosity emitted in the iron line is $(1.1 \pm 0.1) \times 10^{36}$ ergs s^{-1}.

c) *Distribution of the Continuum Emission*

We tried a model convolution fit to the scan profiles of the Galactic center region in the continuum energy bands of 4.5–9.2 keV and 9.2–18.5 keV. Contrary to the iron line emission, it is not realistic to determine the surface brightness of the

TABLE 2

SPECTRAL PARAMETERS NEAR THE GALACTIC CENTER

Position		Temperature (keV)	Line Intensity (photons s^{-1} beam^{-1})	Line Energy (keV)	log N_H	Reduced χ^2 (DOF = 18)
l	b					
1.2	0.5.....	14.9 ± 1.0	10.51 ± 0.71	6.59 ± 0.04	21.9 ± 0.1	1.38
1.2	−0.6.....	13.5 ± 1.3	7.00 ± 0.71	6.71 ± 0.06	21.8 ± 0.1	0.80
358.0	−0.6.....	9.8 ± 1.3	4.74 ± 0.75	6.69 ± 0.09	22.1 ± 0.1	0.67
358.0	−1.1.....	9.0 ± 0.7	3.54 ± 0.38	6.84 ± 0.07	22.1 ± 0.1	1.17

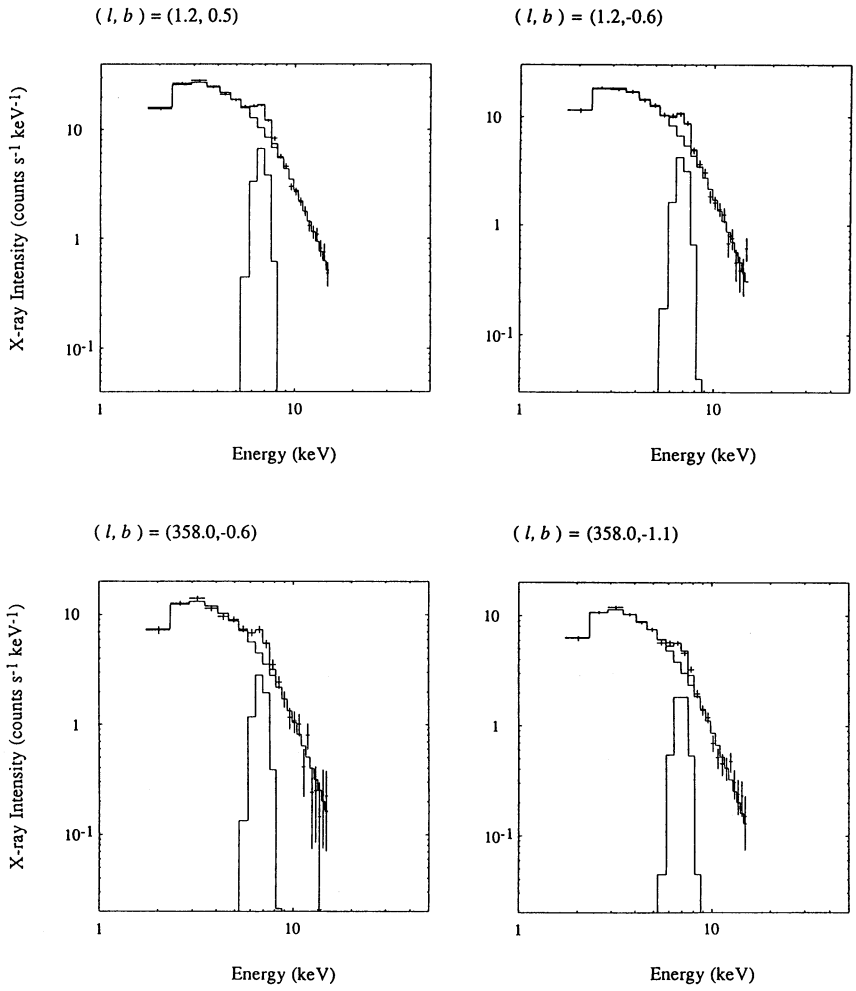

FIG. 1.—The X-ray spectra from the region near the Galactic center where no cataloged X-ray source is in the LAC field of view. The best-fit curves are given by the solid lines in the figure (see text).

extended emission in the continuum X-ray band, because the Galactic center region is crowded with many bright sources (A1742−294, 1E 1740.7−2942, 1E 1743.1−2843, SP 1744.2−2959; see, e.g., Skinner *et al.* 1987; Kawai *et al.* 1988). We therefore assumed that the surface brightness of the continuum X-ray band is proportional to that of the iron emission line. Then we conducted two-dimensional Gaussian fitting including cataloged X-ray sources. The shape of the diffuse emission is fixed to that of the iron line emission, and the positions of cataloged X-ray sources are fixed following Kawai *et al.* (1988). Thus the total intensities of the extended emission and cataloged point sources are left as free parameters. The fitting is generally unacceptable, partly because the intensities of point sources were time-variable and the assumed distribution of the extended X-ray emission is too simplified. The number of point sources which gives a significant contribution to the scan profile is also unclear. Therefore, we tried fitting each scan profile independently in the following manner. At first, we include the one brightest point source. Then we continued the fitting adding a next brightest source and examined the decrease of best-fit reduced χ^2 values. After adding three or four point sources, we found no decrease of the reduced χ^2 value by the inclusion of an additional point source. The final results are given in Table 4. The scatter of the intensity of the extended emission would give a possible uncertainty caused by this model fitting. Thus we regard that the total flux from the extended emission in the 4.5–9.2 keV energy band, with a very rough estimation, is in the range of 200–420 counts s^{-1}. Using the same method we estimate that the flux of the 9.2–18.5 keV band is 60–110 counts s^{-1}. The count ratio in the 4.5–9.2 keV band and the 9.2–18.5 keV band is between 0.14 and 0.35, which corresponds to a temperature range of 5–19 keV under the assumption of a thermal bremsstrahlung spectrum. The surface brightness at the peak is (2–5) $\times 10^{-6}$ ergs s^{-1} cm^{-2} sr^{-1}. The total flux and luminosity are (1–3) $\times 10^{-9}$ ergs s^{-1} cm^{-2}, and (0.9–3) $\times 10^{37}$ ergs s^{-1} in the 2–10 keV energy band, respectively. The equivalent width of the iron line is estimated to be 500–1300 eV. This is roughly consistent with the value expected from a thin hot plasma with cosmic abundance, at a temperature of about 10 keV in collisional ionization equilibrium (Raymond and Smith 1977).

IV. DISCUSSION

Extended X-ray emission near the Galactic center has been reported with the *Einstein Observatory* (Watson *et al.* 1981), the SPARTAN 1 mission (Kawai *et al.* 1988), and the Spacelab 2 mission (Skinner *et al.* 1987). For a quantitative comparison of the present result with those of previous observations, we list the present result of the Galactic center emission as well as those of the previous observations in Table 5, where the total

TABLE 3

IRON LINE DISTRIBUTION IN THE GALACTIC CENTER REGION

A. $b = 1.^\circ7$

l	Iron Line Intensity (photons s^{-1} $beam^{-1}$)	Line Energy (keV)	Reduced χ^3 DOF = 8
$-5.^\circ0$ to $-4.^\circ2$....	2.45 ± 0.41	6.68 ± 0.10	1.17
−4.2 to −3.4....	1.89 ± 0.57	6.64 ± 0.18	1.23
−3.4 to −2.6....	1.64 ± 0.25	6.54 ± 0.11	1.96
−2.6 to −1.8....	1.34 ± 0.61	6.59 ± 0.22	0.60
−1.0 to −0.2....	3.22 ± 0.41	6.80 ± 0.08	1.30
−0.2 to 0.6....	4.28 ± 0.47	6.81 ± 0.06	1.60
0.6 to 1.4....	3.39 ± 0.44	6.88 ± 0.08	0.68
3.4 to 4.2....	0.62 ± 0.21	6.65 ± 0.23	0.89
4.2 to 5.0....	1.68 ± 0.43	6.80 ± 0.14	1.09

B. $b = 0.^\circ5$

l	Iron Line Intensity (photons s^{-1} $beam^{-1}$)	Line Energy (keV)	Reduced χ^2 DOF = 12
$-4.^\circ2$ to $-3.^\circ4$....	2.52 ± 0.31	6.88 ± 0.08	1.14
−3.0 to −2.6....	3.04 ± 0.48	6.73 ± 0.10	1.09
−2.6 to −2.2....	2.58 ± 0.54	6.77 ± 0.13	1.22
−2.2 to −1.8....	3.67 ± 0.55	6.71 ± 0.09	0.63
−1.8 to −1.4....	5.42 ± 0.71	6.69 ± 0.08	1.14
−1.4 to −1.0....	8.55 ± 0.99	6.69 ± 0.06	1.38
−1.0 to −0.6....	14.30 ± 1.54	6.66 ± 0.06	1.40
−0.6 to −0.2....	16.55 ± 1.94	6.64 ± 0.07	1.14
−0.2 to 0.2....	20.87 ± 1.63	6.74 ± 0.04	1.33
0.2 to 0.6....	19.54 ± 1.38	6.66 ± 0.04	0.44
0.6 to 1.0....	16.03 ± 1.09	6.61 ± 0.04	1.57
1.0 to 1.4....	10.39 ± 0.79	6.59 ± 0.05	1.11
3.2 to 3.6....	3.93 ± 1.01	6.62 ± 0.14	0.93
3.6 to 4.0....	2.69 ± 0.25	6.69 ± 0.06	0.96

C. $b = -0.^\circ6$

l	Iron Line Intensity (photons s^{-1} $beam^{-1}$)	Line Energy (keV)	Reduced χ^2 DOF = 11
$-3.^\circ8$ to $-3.^\circ4$....	2.80 ± 0.56	6.48 ± 0.11	0.79
−3.4 to −3.0....	3.19 ± 0.65	6.59 ± 0.12	0.95
−2.6 to −2.2....	3.73 ± 0.68	6.55 ± 0.11	0.58
−2.2 to −1.8....	4.51 ± 0.83	6.71 ± 0.11	0.69
−1.8 to −1.4....	4.70 ± 0.91	6.84 ± 0.11	1.16
−1.4 to −1.0....	9.51 ± 1.25	6.71 ± 0.08	1.89
−1.0 to −0.6....	14.24 ± 2.63	6.42 ± 0.10	1.31
−0.6 to −0.2....	15.80 ± 2.39	6.61 ± 0.09	0.27
−0.2 to 0.2....	20.06 ± 1.58	6.68 ± 0.04	0.56
0.2 to 0.6....	15.81 ± 1.29	6.67 ± 0.05	0.56
0.6 to 1.0....	10.95 ± 0.84	6.67 ± 0.04	2.09
1.0 to 1.4....	6.87 ± 0.76	6.73 ± 0.06	0.72
1.4 to 1.8....	4.50 ± 0.83	6.78 ± 0.10	1.65
3.0 to 3.4....	2.80 ± 0.58	6.74 ± 0.11	0.73
3.4 to 3.8....	2.12 ± 0.42	6.68 ± 0.12	1.14

D. $b = -1.^\circ1$

l	Iron Line Intensity (photons s^{-1} $beam^{-1}$)	Line Energy (keV)	Reduced χ^2 DOF = 11
$-5.^\circ0$ to $-4.^\circ6$....	2.46 ± 0.51	6.71 ± 0.12	0.87
−4.6 to −4.2....	2.60 ± 0.40	6.79 ± 0.09	0.45
−4.2 to −3.8....	2.13 ± 0.42	6.68 ± 0.11	0.47
−3.8 to −3.4....	3.12 ± 0.44	6.69 ± 0.08	1.13
−3.4 to −3.0....	2.96 ± 0.50	6.55 ± 0.10	1.04
−3.0 to −2.6....	3.14 ± 0.38	6.76 ± 0.08	1.48
−2.6 to −2.2....	3.13 ± 0.41	6.69 ± 0.08	1.01
−2.2 to −1.8....	3.57 ± 0.40	6.84 ± 0.07	1.55
−1.8 to −1.4....	3.90 ± 0.55	6.68 ± 0.08	0.68
−1.4 to −1.0....	6.68 ± 0.94	6.62 ± 0.08	1.21
−1.0 to −0.6....	11.88 ± 1.33	6.53 ± 0.06	0.80
−0.6 to −0.2....	12.48 ± 1.38	6.55 ± 0.06	1.74
−0.2 to 0.2....	11.22 ± 1.14	6.59 ± 0.06	1.18
0.2 to 0.6....	10.35 ± 0.83	6.72 ± 0.04	0.81
0.6 to 1.0....	6.48 ± 0.66	6.65 ± 0.06	1.51

TABLE 3—*Continued*

D. $b = -1.^\circ1$

l	Iron Line Intensity (photons s^{-1} $beam^{-1}$)	Line Energy (keV)	Reduced χ^2 DOF = 11
1.0 to 1.4....	4.39 ± 0.59	6.60 ± 0.08	1.21
1.4 to 1.8....	4.01 ± 0.44	6.66 ± 0.07	1.44
1.8 to 2.2....	3.73 ± 0.48	6.85 ± 0.08	1.63
2.2 to 2.6....	2.86 ± 0.74	6.67 ± 0.13	1.01
2.6 to 3.0....	3.24 ± 0.36	6.69 ± 0.06	1.58
3.0 to 3.4....	2.75 ± 0.38	6.76 ± 0.08	0.93
3.4 to 3.8....	1.77 ± 0.43	6.72 ± 0.14	0.64

E. $b = -2.^\circ1$

l	Iron Line Intensity (photons s^{-1} $beam^{-1}$)	Line Energy (keV)	Reduced χ^2 DOF = 8
$-5.^\circ0$ to $-4.^\circ2$....	1.40 ± 0.27	6.82 ± 0.11	1.30
−4.2 to −3.4....	1.72 ± 0.36	6.79 ± 0.12	0.65
−3.4 to −2.6....	1.39 ± 0.61	6.51 ± 0.23	0.92
−2.6 to −1.8....	1.77 ± 0.59	6.77 ± 0.18	0.77
−1.8 to −1.0....	2.47 ± 0.35	6.70 ± 0.08	1.52
−0.6 to −0.2....	2.91 ± 0.65	6.58 ± 0.13	0.56
−0.2 to 0.2....	2.65 ± 0.49	6.69 ± 0.11	2.82
0.2 to 0.6....	2.87 ± 0.54	6.69 ± 0.11	1.57
0.6 to 1.0....	2.46 ± 0.22	6.91 ± 0.06	1.74
1.0 to 1.8....	2.04 ± 0.29	6.87 ± 0.09	0.62
1.8 to 2.6....	1.77 ± 0.31	6.78 ± 0.10	1.56
2.6 to 3.4....	1.73 ± 0.38	6.74 ± 0.13	0.50
3.4 to 4.2....	1.69 ± 0.34	6.75 ± 0.12	1.76

flux and the surface brightness are converted to those of the same energy band of 2–10 keV using the spectral shape determined in § III. Since the energy range of the *Einstein* data was limited below a few keV, we did not list the *Einstein* result. Kawai *et al.* (1988) found that the extended emission had an elliptical shape (axial ratio ~0.41) with a major axis tilted by ~18° with respect to the Galactic plane, while Skinner *et al.* (1987) reported that the extended emission is roughly spherical. Our present results support Kawai *et al.* (1987). Although the reported peak fluxes are not much different from each other, the total flux and the size of the emission region detected in the *Ginga* observations are significantly larger than those obtained during the previous observations. This conflict should be due to a difference in the surface brightness detection limit. The better sensitivity of the *Ginga* instrument allows the detection of a larger spatial extension and hence results in a larger total flux compared to the previous experiments.

The most important result of the present observation is the detection of iron line emission at 6.7 keV from the extended region near the Galactic center. This, together with the spectral fitting, leads us to conclude that the Galactic center emission is due to thermal emission from an optically thin hot plasma of about 10 keV. The iron line equivalent width of 500–1300 eV suggests that the iron abundance in this plasma is about the same as the cosmic value (Raymond and Smith 1977).

The optically thin thermal spectrum from the Galactic center is quite different from those of typical X-ray binary stars. The emission from binary X-ray stars is generally optically thick (with an absent or very weak 6.7 keV line) due to their compact emission region. If we assume that the accretion rate onto the compact star (neutron star or black hole) becomes very low, we can expect that the emission would become optically thin. However, the temperature would be much higher than 10 keV because of the extremely deep gravitational potential. The potential well of a white dwarf is rea-

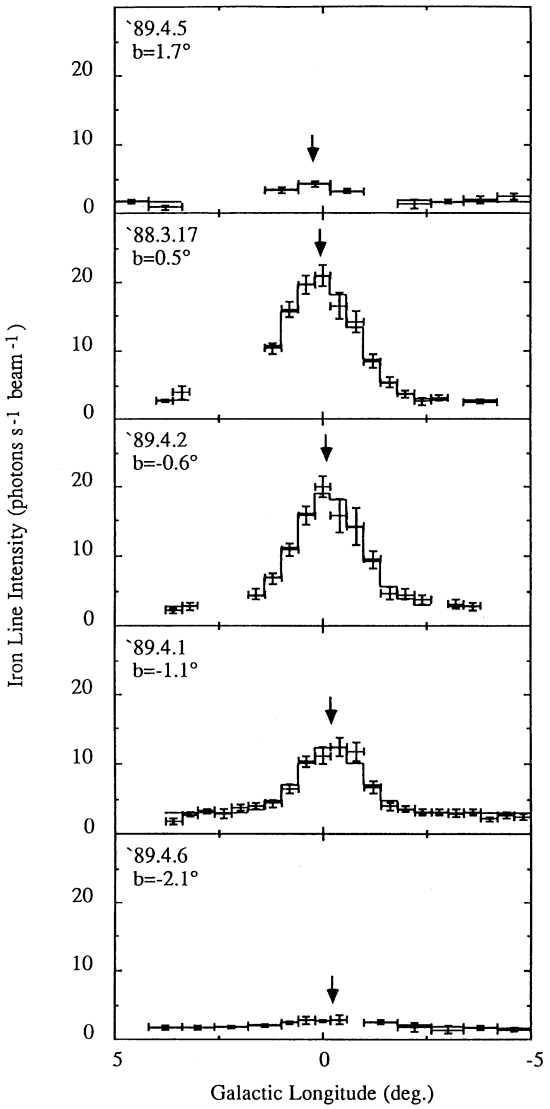

FIG. 2.—The Galactic longitude distribution of the iron line intensity. The solid lines in each panel show the best-fit curve assuming a one-dimensional Gaussian distribution plus constant background. The arrows show the intensity peak of each profile. The intensity peak shows a systematic shift from the Galactic center.

sonably deep, and from an accreting white dwarf we can expect an optically thin thermal spectrum with $kT \sim 10$ keV. Other candidate sources with a same sort of spectrum are RS CVn systems and star-forming regions. The other possibility is that the emission is due to diffuse plasma extending to as large as several hundred pc. This plasma could be produced by shock heating, e.g., related to a large explosion and/or multiple supernova explosions. In what follows we discuss the origin of the Galactic center plasma in more detail.

a) Integrated Emission of Discrete Sources

The X-ray spectrum of white dwarf binaries (cataclysmic variables; CVs) and RS CVn systems are known to be thermal. We will discuss whether the spectrum, in particular the iron line feature, is similar to that observed for the extended Galactic center source. Unfortunately accurate X-ray spectra of CVs and RS CVn systems in the energy range above 2 keV are still sparse. Recent *Ginga* observations of RS CVn systems and CVs suggest that the iron equivalent width for these objects are generally smaller than that expected from cosmic abundance (Tsuru *et al.* 1989; M. Ishida 1990, private communication). Furthermore the iron energy from CVs derived from the *Ginga* observations is not always 6.7 keV but shows rather lower values, ranging from 6.4 to 6.5 keV (M. Ishida 1990, private communication). From these facts we conclude that the CVs and RS CVn systems are not a major contributor to the Galactic center emission. Independently of this, it would be difficult to reconcile our results with the spatial distribution of CVs and RS CVn systems near the Galactic center: if these objects follow the distribution of normal stars distribution (Genzel and Townes 1987), the surface brightness caused by these objects should not show a tilted elliptical structure as obtained from the Galactic center observation.

b) Star-forming Regions: Supernova or Nova Explosions

We propose that a more plausible candidate is the integrated emission from many star-forming regions. Although we have not enough X-ray data to estimate this contribution, we note that typical star-forming regions, such as the Orion Nebula, the ρ Oph Dark Cloud, and the η Car nebula, show spectra similar to the Galactic center emission (Agrawal *et al.* 1986; Koyama 1987; Becker *et al.* 1976; Koyama *et al.* 1990). The tilted surface brightness of the Galactic center emission may be explained if many star-forming regions are associated with molecular clouds around the Galactic center because the distribution of the molecular clouds is not symmetrical but shows the similar tilted structure (e.g., Sofue 1989). Since the typical luminosity of one star-forming region is of order 10^{33} ergs s^{-1}, 10^4 star-forming regions are required within several hundred pc of the Galactic center.

The young supernova remnants, which have a thermal spectrum with an intense iron line, are similar spectra as the Galactic center emission. Since the observed temperature is as high

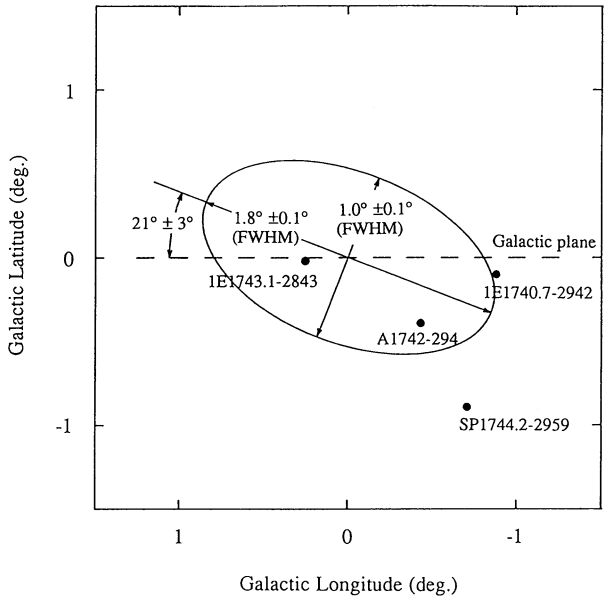

FIG. 3.—The iron line–emitting region in the Galactic center region superposed on the SPARTAN 1 point sources (Kawai *et al.* 1988). The distribution is interpreted as a tilted two-dimensional Gaussian.

TABLE 4

RESULTS OF FITTING OF CONTINUUM SCAN PROFILES IN 4.5–9.2 keV/9.2–18.5 keV BANDS

Date	Diffuse Emission (counts s^{-1})	A1742−294 (counts s^{-1})	1E 1743.1−2843 (counts s^{-1})	SP 1744.2−2959[a] and 1E 1740.7−2942 (counts s^{-1})
1988 Mar 17	286 ± 8	250 ± 13	56 ± 4	101 ± 49
	86 ± 4	67 ± 8	18 ± 3	108 ± 36
1989 Apr 1	300 ± 13	98 ± 3	15 ± 7	122 ± 6
	105 ± 8	25 ± 3	0 ± 8	53 ± 8
1989 Apr 2	198 ± 10	124 ± 4	44 ± 5	132 ± 5
	60 ± 7	32 ± 3	17 ± 4	61 ± 3
1989 Apr 5	284 ± 14	...[b]	91 ± 23	29 ± 22[c]
	61 ± 13	...[b]	0 ± 9	65 ± 17[c]
1989 Apr 6	423 ± 31	194 ± 19	...[b]	33 ± 4[d]
	61 ± 21	65 ± 13	...[b]	13 ± 3[d]

NOTE.—The upper row shows the count rate in the 4.5–9.2 keV band and the lower, in the 9.2–18.5 keV band.

[a] We show the sum of the point source intensities because we cannot distinguish between the flux from SP 1744.2−2959 and that from 1E 1740.7−2942 due to small separation in azimuthal angle.

[b] This source is out of the field of view.

[c] SP 1744.2−2959 is out of the LAC field of view.

[d] 1E 1740.7−2959 is out of the LAC field of view.

as about 10 keV, these supernova remnants should be very young (e.g., less than 10^3 yr depending on the ambient density) or the ambient density should be very low (Sedov 1959). The latter case is discussed in more detail in the next subsection. A typical young supernova remnant younger than 10^3 yr old, such as the Kepler or Tycho supernova remnant, has an X-ray flux of about 10^{-10} to 10^{-11} ergs cm^{-2} s^{-1} with an angular size of a few arcminutes at the Galactic center (Seward 1990). Since this flux and size could have been resolved with previous experiments, we conclude that typical young supernova remnants are not a major contributor to the Galactic center emission.

On the other hand, supernova remnants in a tenuous medium have high temperature for a long time and their X-ray surface brightness would be very low. Therefore, these supernova remnants would escape detection of previous experiments. We will discuss this case in § IV*c*.

A scaled-down version would be the integrated emission of a large number of nova explosions. Since we do not have enough data in hand on the X-ray emission from nova explosions and since the rate of nova occurrence near the Galactic center is not well known, we are not able to discuss this possibility quantitatively. However, for the following reason we suspect that nova explosions are not important. The spatial distribution of novae would be similar to those of the normal stellar distribution rather than those of young objects such as the molecular cloud and the star-forming region. The stellar distribution determined by infrared observation (Genzel and Townes 1987) does not show a tilted elliptical shape, which is in conflict with the shape of the extended X-ray emission.

c) Energetic Explosions at the Galactic Center

To study the case of multiple supernova explosions in a tenuous ambient medium, we will assume that the density of the hot gas is uniform over the entire region of the Galactic center emission. Using the parameters listed in Table 5 and the bremsstrahlung emission rate at $kT = 10$ keV, we find that the emission measure is given to be (4–12) × 10^{59} cm^{-3}. Assuming axial symmetry around the major axis of the extended emission, we estimate the volume to be about 3 × 10^{62} cm^3. Correspondingly, the electron density of the diffuse plasma is 0.03–0.06 cm^{-3}. The total thermal energy in this volume is $E_{th} = 3n_e kTV \sim$ (4–8) × 10^{53} ergs s^{-1} and the total mass of hot gas is (1–2) × 10^4 $M_\odot$. These values correspond to those of about 10^3 supernova explosions. The cooling time is $\sim 10^9$ yr, while the typical time scale of the plasma (obtained by dividing its diameter by the sound velocity) is $\sim 10^5$ yr. Since the gas temperature is very high, the plasma is not gravitationally

TABLE 5

OBSERVED PARAMETERS OF THE THIN HOT PLASMA

Parameter	*Ginga*	SPARTAN 1[a]	Spacelab 2[b]
Shape	Elliptical	Eliptical	Roughly Circular
Angular size	Major axis 1°.8 Minor axis 1°.0 (FWHM)	Major axis 1°.27 Minor axis 0°.52 (FWHM)	Radius 1°.0 (Full width at zero intensity)
Iron line emission:			
Surface brightness (ergs s^{-1} cm^{-2} sr^{-1})	(2.2 ± 0.1) × 10^{-7}	...	...
Total flux (ergs s^{-1} cm^{-2})	(1.3 ± 0.1) × 10^{-10}	...	...
Continuum emission of the plasma (2–10 keV):			
Surface brightness (ergs s^{-1} cm^{-2} sr^{-1})	(2–5) × 10^{-6}	(1.5 ± 0.1) × 10^{-6}	(2.4 ± 0.1) × 10^{-6}[c]
Total flux (ergs s^{-1} cm^{-2})	(1–3) × 10^{-9}	(3.4 ± 0.3) × 10^{-10}	(7.0 ± 0.3) × 10^{-10}[c]

[a] Kawai *et al.* 1988.

[b] Skinner *et al.* 1987.

[c] Converted to 2–10 keV energy band assuming the thermal bremsstrahlung with the temperature of 10 keV.

bound and the latter time scale should provide a reasonable upper limit to its age. This suggests that multiple supernova explosions (about 10^3 SN) or, alternatively, an energetic explosion of about 10^{54} ergs took place in the Galactic center region during the last 10^5 yr. We note that von Ballmoos, Diehl, and Schönfelder (1987) detected a ^{26}Al γ-ray line near the Galactic center, which is produced in nuclear reactions during energetic phenomena such as supernovae. Our result gives independent support for the occurrence of such energetic explosions near the Galactic center. The outflow of the hot gas would be blocked by a strong magnetic field or a dense cloud. Therefore, the observed asymmetry can be explained by the distribution of dense clouds as discussed by Sofue (1989).

In conclusion, we have discovered an extended optically thin hot plasma with an elliptical shape at the Galactic center. As possible origins of this hot plasma, we propose the integrated emission of star-forming regions, supernova explosions in the tenuous ambient medium or a single large explosion at the Galactic center. However, definite conclusions have to wait for further missions of high spatial resolution such as ASTRO-D and AXAF.

We are grateful to all the members of the *Ginga* team for various support during this work. Thanks are also due to J. van Paradijs and C. Day for a critical reading of the manuscript. The data analysis has been carried out with the FACOM 380 computer at the High Energy Physics Laboratory of Nagoya University.

REFERENCES

Agrawal, P. C., Koyama, K., Matsuoka, M., and Tanaka, Y. 1986, *Pub. Astr. Soc. Japan*, **38**, 723.
Awaki, H., Koyama, K., Kunieda, H., Tawara, Y., and Takano, S. 1991, *Ap. J.*, in press.
Becker, R. H., Boldt, E. A., Holt, S. S., Pravdo, S. H., Rothschild, R. E., Serlemitsos, P. J., and Swank, J. H. 1976, *Ap. J. (Letters)*, **209**, L65.
Genzel, R., and Townes, C. H. 1987, *Ann. Rev. Astr. Ap.*, **25**, 377.
Kawai, N., Fenimore, E. E., Middleditch, J., Cruddace, R. G. Fritz, G. G., Snyder, W. A., and Ulmer, M. P. 1988, *Ap. J.*, **330**, 130.
Koyama, K. 1987, *Pub. Astr. Soc. Japan*, **39**, 245.
———. 1989, *Pub. Astr. Soc. Japan*, **41**, 665.
Koyama, K., Asaoka, I., Ushimaru, N., Yamauchi, S., and Corbet, R. H. D. 1990, *Ap. J.*, in press.
Koyama, K., Awaki, H., Kunieda, H., Takano, S., Tawara, Y., Yamauchi, S., Hatsukade, I., and Nagase, F. 1989, *Nature*, **339**, 603.
Koyama, K., Makishima, K., Tanaka, Y., and Tsunemi, H. 1986, *Pub. Astr. Soc. Japan*, **38**, 121.
Makino, F., and ASTRO-C Team 1987, *Ap. Letters Comm.*, **25**, 223.
Makino, F. 1988, *IAU Circ.*, No. 4571.
Oort, J. H. 1977, *Ann. Rev. Astr. Ap.*, **15**, 295.
Raymond, J. C., and Smith, B. W. 1977, *Ap. J. Suppl.*, **35**, 419.
Sedov, L. I. 1959, *Similarity and Dimensional Methods in Mechanics* (New York: Academic).
Seward, F. D. 1990, *Ap. J. Suppl.*, **73**, 781.
Skinner, G. K., *et al.* 1987, *Nature*, **330**, 544.
Sofue, Y. 1989, *Ap. Letters Comm.*, submitted.
Tsuru, T., *et al.* 1989, *Pub. Astr. Soc. Japan*, **41**, 679.
Turner, M. J. L., *et al.* 1989, *Pub. Astr. Soc. Japan*, **41**, 345.
von Ballmoos, P., Diehl, R., and Schönfelder, V. 1987, *Ap. J.*, **318**, 654.
Watson, M. G., Willingale, R., Grindlay, J. E., and Herts, P. 1981, *Ap. J.*, **250**, 141.

I. HATSUKADE: Department of Electronic Engineering, Faculty of Engineering, Miyazaki University, 1-1 Gakuenkibanadai-nishi, Miyazaki, 889-21, Japan

M. KAWADA, K. KOYAMA, H. KUNIEDA, Y. TAWARA, and S. YAMAUCHI: Department of Astrophysics, School of Science, Nagoya University, Furo-cho, Chikusa-ku, Nagoya, 464-01, Japan